



Modelling of ultrasonic impact treatment (UIT) of welded joints and its effect on fatigue strength

K.L. Yuan, Y.Sumii

Yokohama National University, Japan

sumii@ynu.ac.jp

ABSTRACT. Ultrasonic impact treatment (UIT) is a remarkable post-weld technique applying mechanical impacts in combination with ultrasound into the welded joints. In the present work, a 3D simulation method including welding simulation, numerical modelling of UIT-process and an evaluation of fatigue crack growth has been developed. In the FE model, the actual treatment conditions and local mechanical characteristics due to acoustic softening are set as input parameters. The plastic deformation and compressive stress layer are found to be more pronounced when acoustic softening takes place. The predicted internal residual stress distributions of welded joint before and after UIT are compared with experimental results, showing a fairly good agreement with each other. Finally, simulated results of fatigue crack growth in various residual stress fields are well compared with test results, so that the proposed model may provide an effective tool to simulate UIT-process in engineering structures.

KEYWORDS. UIT; Residual stress; FEM; Surface crack growth.

INTRODUCTION

It is well known that the fatigue strength of steel plates increases in proportion to its static strength. On the other hand, the fatigue strength of the welded joints is little influenced by the static strength level because of the tensile welding residual stress and high stress concentration near the weld toe. Ultrasonic impact treatment (UIT) is a new method for increasing fatigue strength by improving the weld toe geometry, removing defects and introducing beneficial compressive residual stress [1-3]. Recently, new IIW guidance on fatigue strength improvement using high frequency mechanical impact (HFMI) methods including UIT has been prepared by Marquis et al. [4-5]. In parallel to the development of IIW guideline, ship classification societies have also accepted or investigated the UIT as post-weld treatments in ship and offshore structures [6-7].

In order to better understand the effects of UIT on fatigue performance of welded joints, its mechanism has been experimentally investigated in several studies. Cheng et al. [2] measured the residual stress induced by UIT using both X-ray and neutron diffraction (ND) techniques for the first time. The compressive stress layer was found not less than 1mm in depth for welded specimen. A German research project [8, 9] has presented the experimental data that the compressive residual stress is generated down to a depth of 1.5 to 2 mm with maximum values at approximately 0.4 to 0.5 mm below the surface. After treatment the weld toe radius is averaged by 1.5 to 2 mm with its groove depth of 0.1 to 0.2 mm. The study at the University of Waterloo, Canada [10, 11] was carried out to investigate the fatigue performance of structural steel welds subjected to UIT at under-, proper and over-treatment levels, respectively. A close relationship was found between the measured groove depth and local residual stress, indicating the groove depth as an important quality control

parameter. Ultrasonic impact treatment consists of ultrasonic waves and mechanical impacts. Very limited studies [12-14] have demonstrated that the ultrasonic vibration superimposed by UIT on metals has indeed an acoustic softening effect on material properties undergoing deformation.

Normally the experimental methods for residual stress measurements need considerable cost, time and skillful technique. It is practically impossible to obtain full field measurement of residual stress. For this reason, the residual stress induced by UIT has been recently evaluated by some studies using finite element (FE) analysis. There are mainly two groups of simulation methods for UIT process: quasi-static implicit and dynamic explicit methods. The former is modelled as pressing the pin at the weld toe to one prescribed depth by displacement or load control approaches, rather than peening [15-16]. In the latter [17-18], the modelled pin impacts to a symmetry-cell model that is widely used in shot peening simulation [19], however, the welding residual stress is not taken into account. It is found that the predicted in-depth residual stress and groove depth could not consist well with measurements together [15-16], because in the above mentioned simulations the acoustic softening effect has not been introduced, which plays an important role in the mechanism of UIT.

Therefore in this study, one novel 3D prediction approach including thermal-mechanical welding simulation, dynamic elastic-plastic FE analysis of UIT-process, and an evaluation of surface fatigue crack growth for cruciform weld joint has been proposed. The actual process parameters and ultrasonic induced material softening, which is appropriately adjusted to fit experimental results, are considered. The predicted residual stresses distributions, treated weld toe shape and fatigue strength are compared with published test data [3, 20].

THE UIT PROCESS

As depicted in Fig.1, the ultrasonic impact treatment method is based on conversion of harmonic oscillations of the ultrasonic transducer into impact pulses at the treated surface. In order to efficiently transfer the energy into the work piece, the installed cylindrical pins can freely move in a gap between the waveguide end and treated surface. This kind of high frequency impacts of the pin in the combination with the ultrasonic stress waves transmitted into the work piece through the pin contacting the treated surface is called as ultrasonic impact [12].

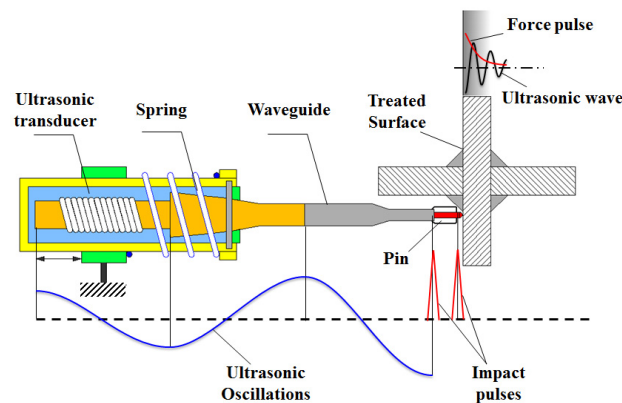


Figure 1: Mechanism of UIT [12].

Model of ultrasonic impact

In order to consider ultrasonic impact phenomenon in numerical simulation, one simplified model based on the description by Statnikov [12, 21] as illustrated in Fig.2 is proposed. During one impact period T_{im} , it comprises both the ultrasonic impact period t_1 and pause between impacts t_2 . In this work, the t_1 is assumed as 1 millisecond, in the case of impact frequency f_{im} of 100Hz and the relation $t_1/T_{im}=0.1$, which is in the range of ultrasonic impact time from hundreds of microseconds to units of milliseconds measured by Statnikov [12]. The oscillations of pin at a frequency of 27 kHz, which mainly cause the plastic deformation, will recur about 30 times during reboundless contact phase up to 1 millisecond.

To construct UIT FE model, the impact velocity of pin during reboundless period is essential. For the impact velocity, it can be assumed here that all the ultrasonic impact on the treated surface will occur at the same velocity and an average

velocity is considered. This average velocity is taken to be the maximum initial velocity of the waveguide. Considering that the sinusoidal harmonic signal delivered by the transducer is

$$x(t) = A \sin(2\pi ft) \tag{1}$$

the maximum initial velocity is

$$V_{\max} = 2\pi fA \tag{2}$$

where A is the maximum displacement amplitude at the waveguide output end and f represents ultrasonic oscillation frequency of UIT.

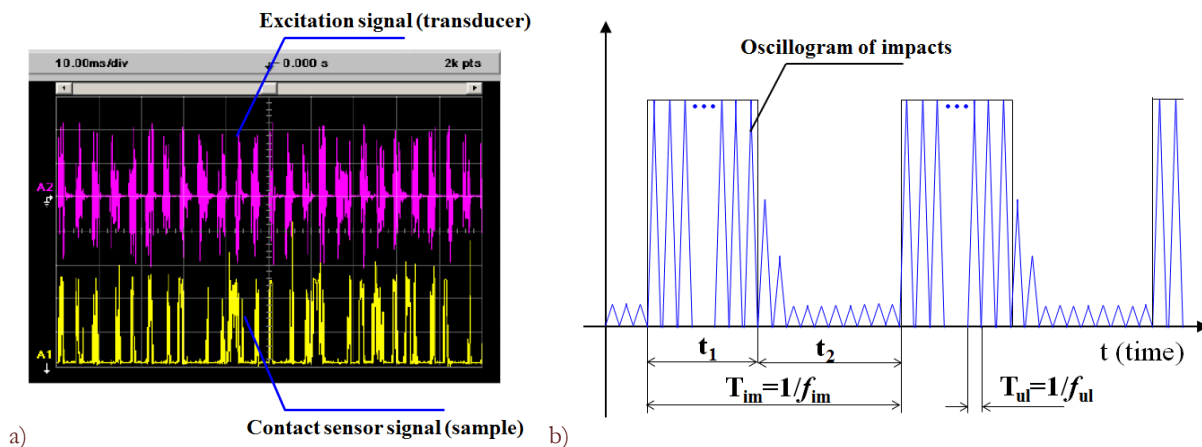


Figure 2: (a) Oscilloscope picture of transducer excitation (top) and ultrasonic impact excitation (bottom) with UIT [12], (b) Model of ultrasonic impact, t_1 -ultrasonic impact length (reboundless), t_2 -pause between ultrasonic impacts (rebounding off), f_{im} -impact frequency, f_{ul} -ultrasonic oscillation frequency, and $t_1/T_{im}=0.1\sim 0.3$ [12], $f_{im}=100\sim 120\text{Hz}$, $f_{ul}=27\sim 44\text{kHz}$ [1].

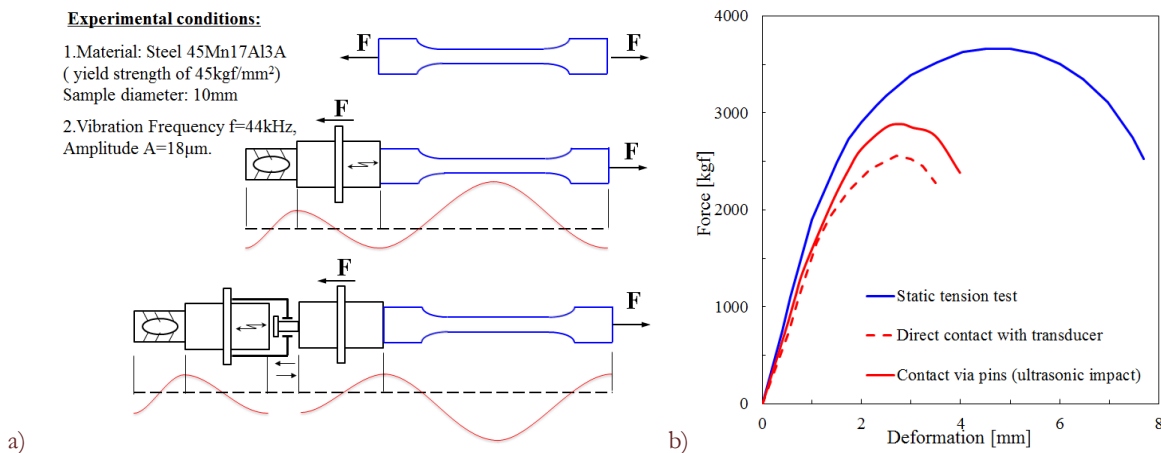


Figure 3: Ultrasonic-assisted tension tests; (a) schematic diagram of test devices with different modes, (b) measured force-deformation data [12].

Acoustic softening effect

The effect of ultrasonic energy on metal deformation behavior for a wide range of metals has been well known since early 1950's [22]. It was observed that the apparent yield strength of the material is immediately reduced upon the application of ultrasonic energy and restores as the removal of ultrasonic energy. As for UIT, the relative motion between the specimen and pin complicates the acoustic softening process. Statnikov [12] performed an ultrasonic-assisted tension test, in order to confirm the effect of ultrasonic impact via an intermediate pin on the deformation resistance reduction in comparison with a direct contact of the ultrasonic transducer and the specimen, as shown in Fig.3. An obvious reduction about 24-



26% in ultimate tensile strength under ultrasonic impact was observed, which is just a little less than the 27-30% reduction in the case of direct ultrasonic action. Nevertheless, the results suggested that the UIT could effectively transfer ultrasound into the treated objects through the area of plastic deformation by means of ultrasonic impact. To the best knowledge of the authors, there is no model to directly quantify the acoustic softening effect related to UIT. Hence, in this work a yield stress reduction parameter η accounting for acoustic softening in Eq.3 is employed. The value of η is iteratively adjusted by comparing the predicted indentation depth with experiment.

$$\sigma_{as} = \sigma_o(1 - \eta) \tag{3}$$

where σ_{as} is the flow stress considering acoustic softening, σ_o is the flow stress without vibration and η ranges from 0 to 1 depending on the amount of acoustic softening.

FINITE ELEMENT MODELING

In the present study, a three dimensional simulation procedure is set up including the uncoupled thermo-mechanical welding simulation by SYSWELD [23], transfer of the results to the initial-stress state of a dynamic model of UIT by explicit method in LS-DYNA [24], as shown in Fig.4.

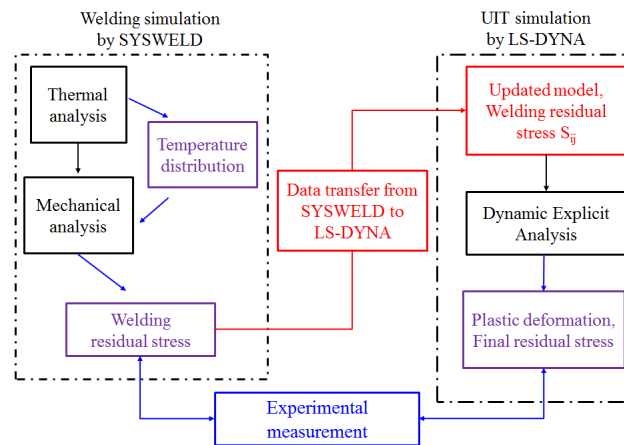


Figure 4: Flowchart of welding-UIT process simulation.

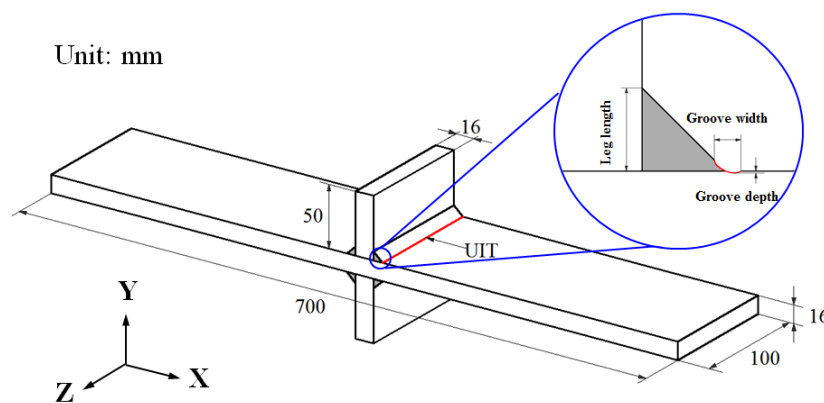


Figure 5: Geometry and dimensions of UIT specimen.

Analysis model and process parameters

A non-load-carrying cruciform joint used in the recent experimental work by Suzuki et al [20] is selected as analysis object. Fig.5 shows the dimensions of test specimen, which was welded using CO₂ fillet welding with JIS-SM490A base metal plate. The welding parameters are given in Tab. 1.

The welded joints for as-weld and UIT were fabricated by one pass welding with leg length of 7mm. The used UIT equipment was Esonix™ 27 UIS. The operating frequency of ultrasonic generator was 27 kHz, shifting speed of 10 mm/s and 3-mm-diameter hardened metal pins.

Welding material	Wire diameter[mm]	Speed [mm/min]	Current [A]	Voltage [V]	Arc efficiency
SF-1	1.2	300	250	29	80%

Table 1: Welding conditions.

Simulation of welding process

For welding simulation, a half symmetrical 3D model of cruciform joint is created. This FE model has been constructed for small width of 4 mm, in order to be most effective considering the accuracy and computational effort (see Fig.6). Therefore both sides of this segment are restrained in Z-direction, to simulate the specimen in plane strain state. The FE model mainly employs 8-node hexahedral solid elements except for few wedge elements in the weld bead region. Near the weld toe, an extremely fine mesh (0.2×0.1×0.2mm) is required for the following UIT process simulation.

In the first step of thermal analysis, heat input (1160 J/mm) is given all at once to the weld metal and an initial temperature of 1400°C for activation of the weld bead material elements is assumed. Accompanying with heat radiation and convection, the cooling-down period between the subsequent weld is set as 1 hour. For the second step of mechanical analysis, the material model is assumed to follow von Mises yield criterion with bilinear kinematic hardening. The used temperature-dependent thermal and mechanical material properties are illustrated in Fig.7.

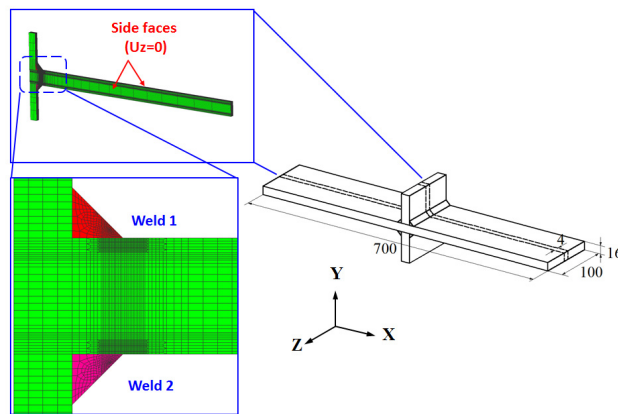


Figure 6: Finite element model for welding simulation.

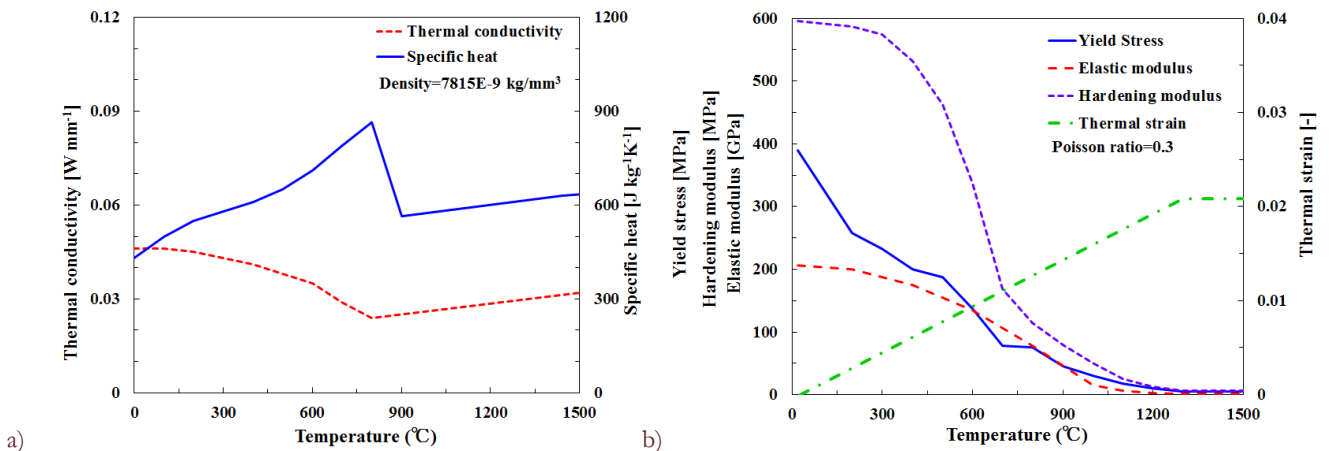


Figure 7: Temperature-dependent material properties referring to SYSWELD material database [23].

Simulation of UIT process

After welding simulation in SYSWELD, the results of cruciform joint including element information, as-weld residual stress distribution and plastic strain are imported into LS-DYNA. The tips of 3-mm-diameter pins are modelled as elastic body with an elastic modulus of 206 GPa, Poisson’s ratio of 0.3 and measured mass of 1.5 gram [16]. The pins are angled at 67.5° to the top and bottom surfaces of the specimen. According to Eq. 2, the impact velocity V_{imp} is estimated as 5m/s with corresponding equipment parameters (oscillation frequency of 27 kHz and amplitude of 30 μm under loaded condition [1]). The pin is controlled to continuously impinge the weld toe at the same location for 30 times (equivalent to one ultrasonic impact as mentioned before) by using restart analysis option of LS-DYNA. After each ultrasonic impact, the pin is moved 0.4 mm along weld line to achieve a smooth peened groove with reasonable calculation efforts. This leads to at least four overlapping indentations for the contact area of pin. The weld toe on the top surface is first peened, and that on the bottom surface is subsequently treated.

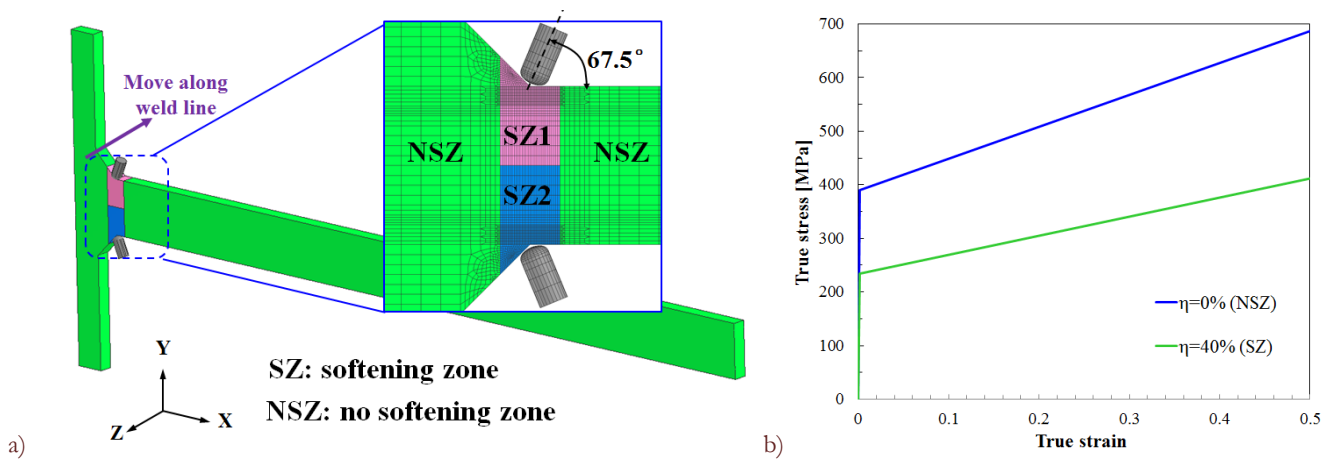


Figure 8: (a) Finite element model of UIT, (b) Mechanical properties considering acoustic softening.

The material of the weld joint is assumed to follow linear kinematic hardening behavior. To consider the acoustic softening effect in Eq.3, the parameter η is selected as 40% by trial and error, so that predicted groove depth fits to the experimental results. The softening zones (SZ) around the weld toe in Fig.8 are assumed to be affected by acoustic softening during peening, of which each depth is determined as 8mm according to measured stress reduction in 16-mm-thickness specimen [14], and the remain zones (NSZ) are not affected by softening. It should be noted that the apparent yield stress dominantly affected by acoustic softening reveals reduction, although the strain-rate effect due to oscillatory stress has been implicitly included in the above mentioned ultrasonic-assisted test [12].

In order to prevent unnecessary long post-impact residual oscillations, which may lead to numerical instability, in this model the material proportional damping is employed as follow:

$$C = \alpha M = 2\omega_0 \xi M \tag{4}$$

$$\omega_0 = \frac{\pi}{2T} \sqrt{\frac{E}{\rho}} \tag{5}$$

where C is the damping matrix, M is the mass matrix, α is the mass proportional Rayleigh damping, ω_0 is the lowest natural frequency, ξ is the corresponding damping ratio, E is elastic modulus, ρ and T are density and thickness of the plate, respectively. According to [19], the adopted value of $\xi=0.5$ is adequate for the rapid stress convergence. Moreover, the contact surfaces are set between the pin tip and the specimen with a Coulomb friction coefficient $\mu=0.5$.

VALIDATION OF WELDING-UIT SIMULATION

Determination of acoustic softening parameter

The acoustic softening parameter η is firstly selected by trial and error so as to match the experimentally measured indentation depth d and weld toe radius r [20] on a cross-section with the predicted ones after one ultrasonic impact, as shown in Fig.9. It can be seen that it is easier to form a smooth change of the shape at the weld toe

when the resistance necessary for plastic deformation is decreased due to acoustic softening, and the parameter, $\eta=40\%$, is used in the following UIT simulation. This result is comparable to the measured yield strength reduction of 45% in stainless steel specimen under direct ultrasonic energy 600 Watt [14], while the consumed power of 27 kHz-type UIT equipment is 600-1200 Watt [1].

The internal residual stress profiles during 30 times of pin's impinging (one ultrasonic impact without translation along weld line) are shown in Fig.10. Near the plate surface the compressive residual stress layer appears. The surface compressive residual stress gradually increases with the peening, but this increase is saturated after 30 times of continuous peening. Having introduced the yield strength reduction due to acoustic softening, the compressive residual stress layer is deepened approximately by 2mm, while the maximum value decreases in comparison with that without acoustic softening (see Fig.10b).

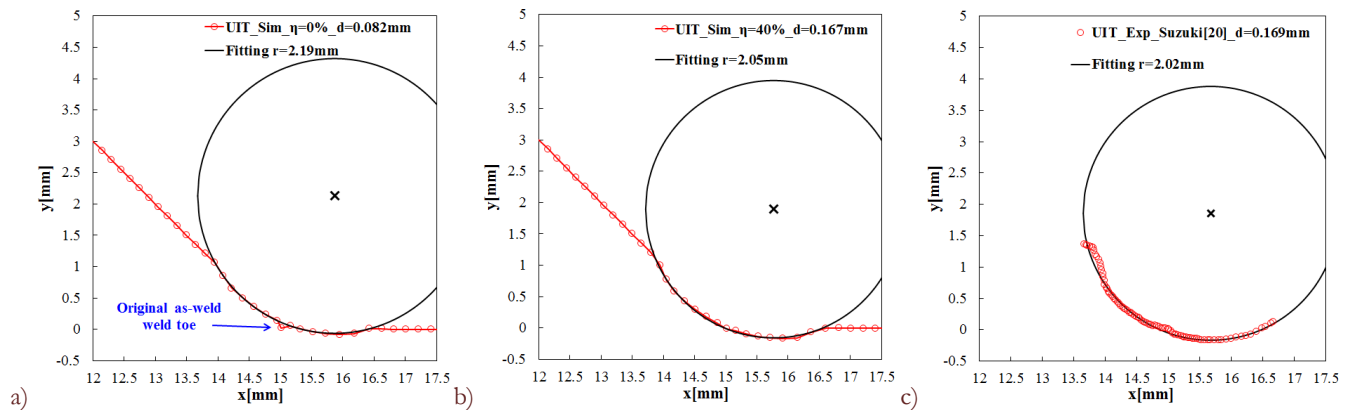


Figure 9: Determination of acoustic softening by comparing the treated weld toe shape; (a) simulated with $\eta=0\%$, (b) simulated with $\eta=40\%$, (c) measured by Suzuki et al. [20].

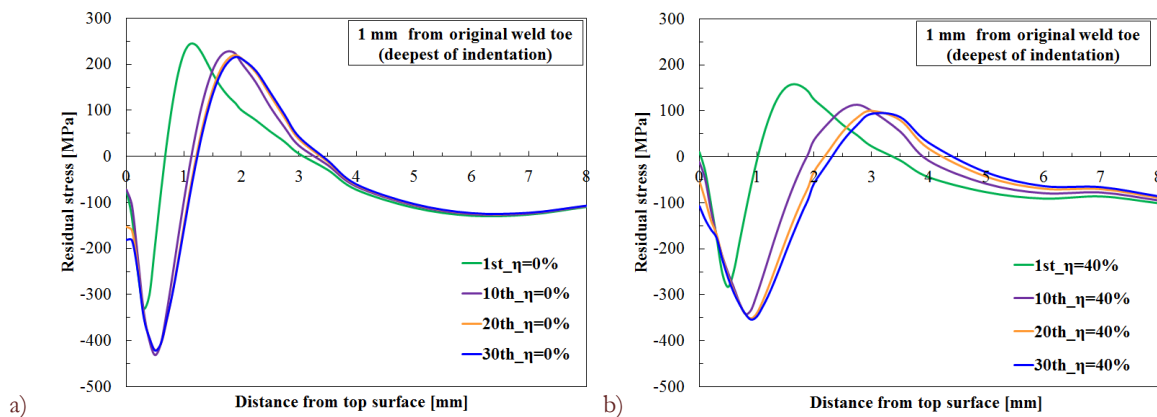


Figure 10: Evolution of in-depth transverse residual stress distributions during one ultrasonic impact; (a) simulated without acoustic softening, (b) simulated with $\eta=40\%$.

Residual stress distribution in the depth direction of As-weld and UIT joints

In practice, the peening tool is travelling along the weld line, until the original shape of the weld toe disappears and the smooth groove is formed. The transverse residual stress σ_x acting perpendicular to the welding line is considered as the driving or resistance force for the surface crack at the weld toe. Therefore, considering the movement of the pin, the transverse residual stress distribution and weld toe shape before and after UIT are illustrated in Fig.11. It has been confirmed that the tensile welding residual stress at the weld toe has been changed to significant compressive residual stress. The step-by-step movement of 0.4 mm provide sufficient overlapping of the impacts. In order to verify the accuracy of the finite element simulation, the residual stress distributions in the depth direction are compared with those measured by X-ray and neutron diffraction methods, respectively [20]. As show in Fig.12, there exist good agreements between the experimental and numerical results. Slight over-estimation of UIT compressive residual stress on the surface



is seen, however, it has been found that the measured surface stress by X-ray method is very sensitive to the location of measurement spot [25].

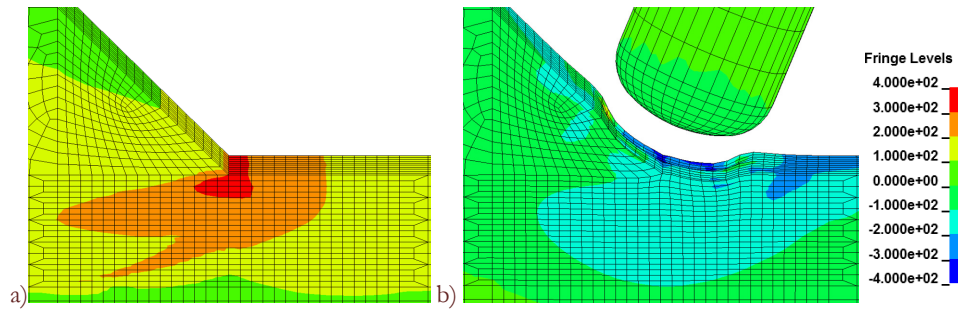


Figure 11: Transverse residual stress distributions and plastic deformation at weld toe; (a) as-weld, (b) UIT with $\eta=40\%$.

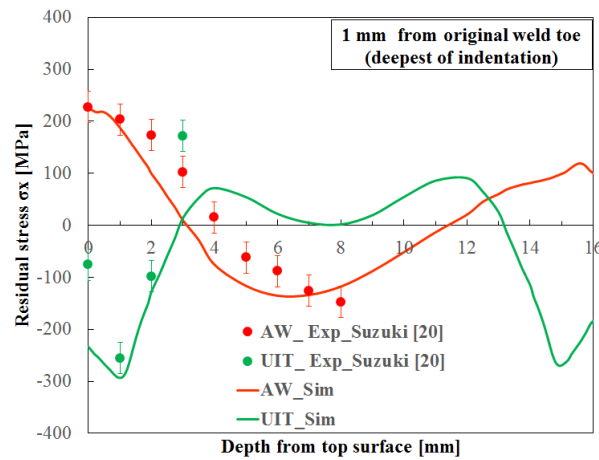


Figure 12: Distribution of transverse residual stress of as-weld and UIT specimens in the depth direction, and comparison with experimental results [20].

FATIGUE LIFE PREDICTION

For accurate fatigue life prediction of a weld joint, it is necessary to consider the stress concentration and residual stress near the weld toe. According to the measurements [20], the weld toe radius r of as-weld and UIT specimen are assumed as 0.25 mm and 2 mm, respectively. The stress concentration factor, K_t , of the weld toe is estimated by the following formula proposed by Tsuji [26]

$$K_t = 1 + [1.348 + 0.397 \ln(\frac{s}{T})] \cdot Q^{0.467} \cdot f_\theta \tag{6}$$

where

$$Q = (l/r) / [2.8(W/T) - 2]$$

$$f_\theta = [1 - \exp(-0.9\sqrt{W/2l} \cdot \theta)] / [1 - \exp(-0.9\sqrt{W/2l} \cdot (\frac{\pi}{2}))]$$

T is the main-plate thickness of 16mm, l is the leg length of 7mm, θ is the flank angle of 45°, and $W=S=T+2l$. Under tension load, the stress distribution near the weld toe is calculated by

$$\sigma_x(y) = \frac{K_t \sigma_n}{2\sqrt{2}} \left[\left(\frac{r}{y+r/2}\right)^{1/2} + \frac{1}{2} \left(\frac{r}{y+r/2}\right)^{3/2} \right] \tag{7}$$



proposed by Glinka [27] in the vicinity of the weld toe taking K_t so obtained by Eq.6 into account, while that apart from the weld toe is calculated by elastic finite element analysis. The symbol used for Eq. 7 and the combined stress distributions are shown in Fig.13, where σ_n represents the nominal stress.

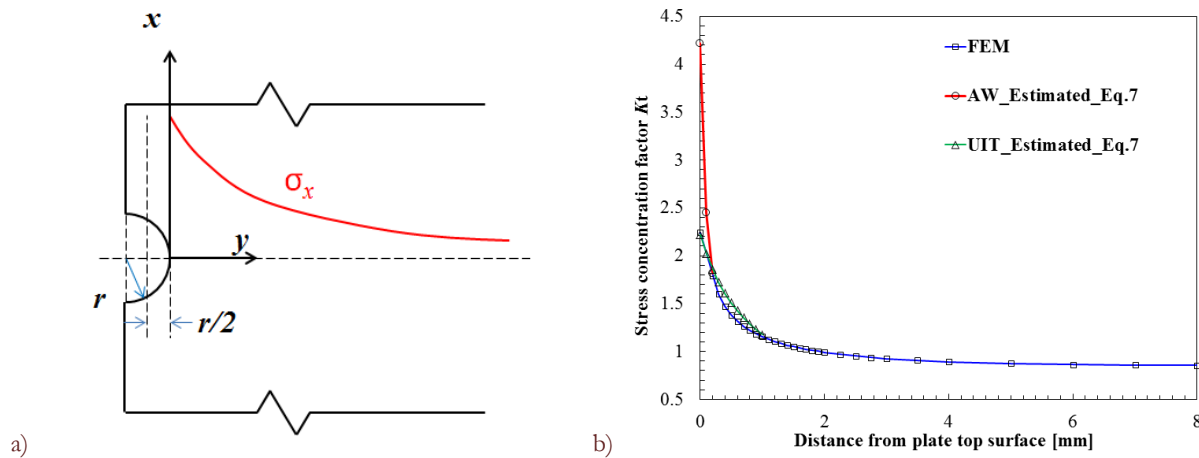


Figure 13: (a) Symbol and coordinate used in Eq.7, (b) Assumed stress concentration near the weld toe.

The stress intensity factors K_I are calculated by

$$K_I = \left[\int_0^a \sigma_x(y) m(y, a) dy \right] \cdot \left[\sec\left(\frac{\pi c}{B} \sqrt{\frac{a}{T}}\right) \right]^{1/2} \quad (8)$$

which is based on the weight function method in code API [28]. Here, the uniform stress distributions in the specimen width direction are assumed, and $m(y, a)$: the weight function which is standardized by the API, $\sigma_x(y)$: the stress distributions, y : distance from surface, a : surface crack depth, c : half crack length, and B : width of specimen.

The crack growth rate of the surface crack at the weld toe is given by

$$da / dN = C [(\Delta K_{eff})^m - (\Delta K_{eff})_{th}^m] \quad (9)$$

based on modified Paris-Elber law using the effective stress intensity range, ΔK_{eff} , and its threshold value, $(\Delta K_{eff})_{th}$. The total and effective stress intensity ranges, ΔK and ΔK_{eff} , are calculated by

$$\Delta K_{eff} = \begin{cases} \Delta K / (1.5 - R_{total}) \\ \Delta K \end{cases} \quad \text{for } \begin{cases} R_{total} < 0.5 \\ R_{total} \geq 0.5 \end{cases}, \quad \text{with } \Delta K = K_{max} - K_{min}, \quad R_{total} = \frac{K_{min} + K_{res}}{K_{max} + K_{res}} \quad (10)$$

where material constants $C=1.45E-11$, $m=2.75$, $(\Delta K_{eff})_{th}=2.45 \text{ MPa}\sqrt{\text{m}}$ according to WES2805[29], R_{total} is the total stress ratio, K_{max} , K_{min} and K_{res} are stress intensity factors for maximum, minimum applied stress and residual stress, respectively.

A single initial semi-circular crack of depth 0.2 mm and final crack depth of $0.8T$ is assumed to propagate at the weld toe in the center of specimen width, referring to the WES recommendation. Fig. 14 shows a comparison of the results of estimations, experiments [3, 20] and recommended FAT-values [4]. These results demonstrate that the proposed fatigue life prediction method clearly distinguishes the difference of fatigue strengths of as-weld and UIT weld joints, by taking the stress concentration and residual stress near the weld toe into account. It should be noted that since multi initial crack followed by crack coalescence are not considered in this work, the present simulation may lead to a slight over-estimation at high applied stress range. In addition, the predicted surface crack shapes are also compared in Fig.14, in which we can clearly observe that the aspect ratio of the UIT case is relatively higher than that of as-weld case because of the compressive residual stress combined with a lower stress concentration factor near the plate surface.

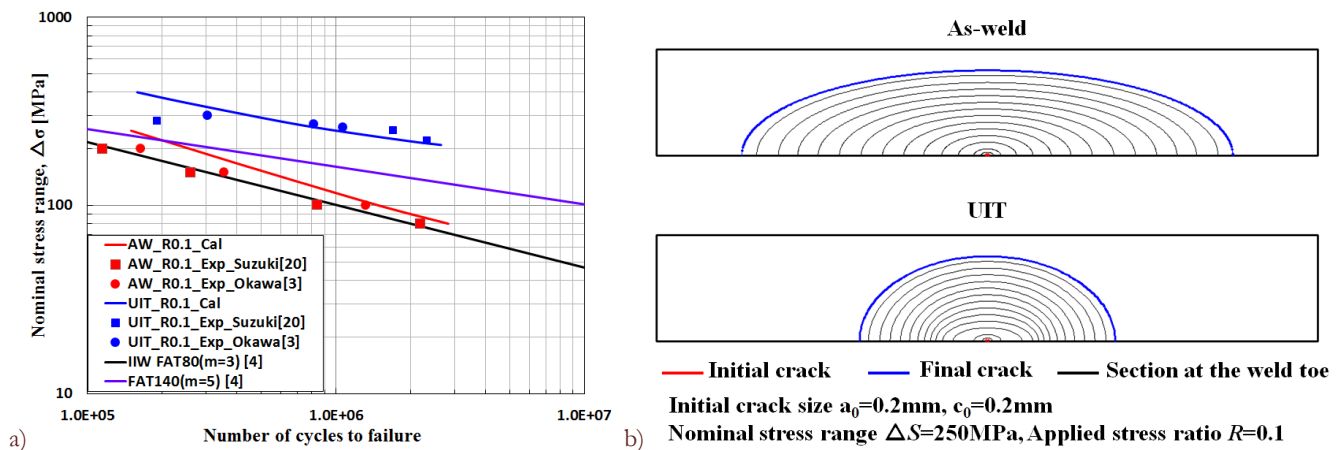


Figure 14: (a) Validation of the predicted fatigue life of the as-weld and UIT joints, (b) Predicted evolution of surface crack shapes.

CONCLUSIONS

Based on the existing experimental observations, a model describing the ultrasonic impact phenomenon is proposed in this paper. Employing commercial codes SYSWELD and LS-DYNA, a three dimensional numerical simulation approaches for UIT-improved welded joints is established, of which the effectiveness has been well validated by comparing with experimental results. From the numerical results, it has been verified that UIT is an effective method to re-distribute the residual stress and reduce the stress concentration near the weld toe area. Deformation and compressive residual stress layer are more pronounced when acoustic softening occurs, which is necessary to be considered in numerical simulation.

ACKNOWLEDGEMENTS

The authors are grateful to Professor Y. Kawamura, Yokohama National University, Dr. H. Shimanuki and Dr. T. Okawa, Nippon Steel & Sumitomo Metal Corporation, for their helpful discussions.

REFERENCES

- [1] Galtier, A., Statnikov, E., The influence of ultrasonic impact treatment on fatigue behavior of welded joints in high-strength steel, *Weld World*, 48 (5-6) (2004) 61-66.
- [2] Cheng, X.H., Fisher, J.W., Prask, H.J., Gnäupel-Herold, T., Yen, B.T., Roy, S., Residual stress modification by post-weld treatment and its beneficial effect on fatigue strength of welded structures, *Int J Fatigue*, 25(9) (2003)1259-1269.
- [3] Okawa, T., Shimanuki, H., Funatsu, Y., Nose, T., Sumi, Y., Effect of preload and stress ratio on fatigue strength of welded joints improved by ultrasonic impact treatment, *Weld World*, 57(2) (2013) 235-241.
- [4] Marquis, G.B., Mikkola, E., Yildirim, H. C., Barsoum, Z., Fatigue strength improvement of steel structures by high-frequency mechanical impact: proposed fatigue assessment guidelines, *Weld World*, 57(6) (2013) 803-822.
- [5] Marquis, G.B., Barsoum, Z., Fatigue strength improvement of steel structures by high-frequency mechanical impact: proposed procedures and quality assurance guidelines, *Weld World*, 58(1) (2014) 19-28.
- [6] American Bureau of Shipping, Commentary on the guide for the fatigue assessment of offshore structures (2014).
- [7] Polezhayeva, H., Howarth, D., Kumar, M., Kang, J. K., Ermolaeva, N., Lee, J.Y., Effect of ultrasonic peening on fatigue strength of welded marine structures-Lloyd's Register Research Programme., *Proc. 24th ISOPE Conference*, (2014) 359-365.
- [8] Weich, I., Edge layer condition and fatigue strength of welds improved by mechanical post-weld treatment, *Weld World*, 55(1-2) (2011) 3-12.



- [9] FOSTA Research Association for Steel Applications, RERRESH-Extension of the fatigue life of existing and new welded steel structures (2011).
- [10] Yekta, R.T., Ghahremani, K., Walbridge, S., Effect of quality control parameter variations on the fatigue performance of ultrasonic impact treated welds, *Int J Fatigue*, 55 (2013) 245-256.
- [11] Ghahremani, K., Safa, M., Yeung, J., Walbridge, S., Haas, C., Dubois, S., Quality assurance for high-frequency mechanical impact (HFMI) treatment of welds using handheld 3D laser scanning technology, *Weld World*, 59(3) (2014) 391-400.
- [12] Statnikov, E., Physics and mechanism of ultrasonic impact treatment, IIW Document 13 (2004) 2004-04.
- [13] Dutta, R.K., Petrov, R.H., Delhez, R., Hermans, M., Richardson, I. M., Böttger, A. J., The effect of tensile deformation by in situ ultrasonic treatment on the microstructure of low-carbon steel, *Acta Materialia*, 61(5) (2013) 1592-1602.
- [14] Gao, H., Dutta, R.K., Huizenga, R.M., Amirthalingam, M., Hermans, M., Buslaps, T., Richardson, I.M., Stress relaxation due to ultrasonic impact treatment on multi-pass welds, *Sci Technol Weld Joining*, 19(6) (2014) 505-513.
- [15] Roy, S., Experimental and analytical evaluation of enhancement in fatigue resistance of welded details subjected to post-weld ultrasonic impact treatment, Diss. Lehigh University, (2006).
- [16] Le Quilliec, G., Lieurade, H. P., Bousseau, M., Drissi-Habti, M., Inglebert, G., Macquet, P., Jubin, L., Mechanics and modelling of high-frequency mechanical impact and its effect on fatigue, *Weld World*, 57.1 (2013) 97-111.
- [17] Yang, X., Zhou, J., Ling, X., Study on plastic damage of AISI 304 stainless steel induced by ultrasonic impact treatment, *Mater Des*, 36 (2012) 477-481.
- [18] Yang, X., Ling, X., Zhou, J., Optimization of the fatigue resistance of AISI304 stainless steel by ultrasonic impact treatment, *Int J Fatigue*, 61 (2014) 28-38.
- [19] Meguid, S. A., Shagal, G., Stranart, J. C., 3D FE analysis of peening of strain-rate sensitive materials using multiple impingement model, *Int J Impact Eng*, 27(2) (2002) 119-134.
- [20] Suzuki, T., Okawa, T., Shimanuki, H., Nose, T., Ohta, N., Suzuki, H., Moriai, A., Effect of ultrasonic impact treatment (UIT) on fatigue strength of welded joints, *Adv Mat Res*, 996 (2014) 736-742.
- [21] Statnikov, E., Method for modifying or producing materials and joints with specific properties by generating and applying adaptive impulses a normalizing energy thereof and pauses there between, U.S. Patent No. 7,301,123 (2007).
- [22] Izumi, O., Oyama, K., Suzuki, Y., Effects of superimposed ultrasonic vibration on compressive deformation of metals, *Trans Jpn Inst Met*, 7(3) (1966) 162-167.
- [23] ESI Group, SYSWELD Ver.2014 (2014).
- [24] Livermore Software Technology Corporation, LS-DYNA Keyword User's Manual Ver. 971 (2007).
- [25] Yildirim, H.C., Marquis, G.B., A round robin study of high-frequency mechanical impact (HFMI)-treated welded joints subjected to variable amplitude loading, *Weld World*, 57(3) (2013) 437-447.
- [26] Tsuji, I., Estimation of stress concentration factor at weld toe of non-load carrying fillet welded joint, *J Soc Naval Architects Jpn*, 80 (1990) 241-251, in Japanese.
- [27] Glinka, G., Calculation of inelastic notch-tip strain-stress histories under cyclic loading. *Eng Fract Mech*, 22(5) (1985) 839-854.
- [28] American Petroleum Institute, API 579-1 Recommended Practice for Fitness-For-Service (2007).
- [29] The Japan Welding Engineering Society, WES 2805 Method of assessment for flaws in fusion welded joints with respect to brittle fracture and fatigue crack growth (1997).